Electron attachment to gas-phase uracil

S. Denifl, S. Ptasińska, G. Hanel, B. Gstir, M. Probst, P. Scheier, and T. D. Märk

Citation: The Journal of Chemical Physics **120**, 6557 (2004); doi: 10.1063/1.1649724
View online: http://dx.doi.org/10.1063/1.1649724
View Table of Contents: http://scitation.aip.org/content/aip/journal/jcp/120/14?ver=pdfcov
Published by the AIP Publishing

Electron attachment to gas-phase uracil

S. Denifl, S. Ptasińska, G. Hanel, B. Gstir, M. Probst, P. Scheier, and T. D. Märk[a)]
Institut für Ionenphysik, Leopold-Franzens Universität Innsbruck, Technikerstr. 25, A-6020 Innsbruck, Austria

(Received 7 October 2003; accepted 30 December 2003)

We present results about dissociative electron attachment (DEA) to gas-phase uracil (U) for incident electron energies between 0 and 14 eV using a crossed electron/molecule beam apparatus. The most abundant negative ion formed via DEA is $(U\text{-}H)^-$, where the resonance with the highest intensity appears at 1.01 eV. The anion yield of $(U\text{-}H)^-$ shows a number of peaks, which can be explained in part as being due to the formation of different $(U\text{-}H)^-$ isomers. Our results are compared with high level *ab initio* calculations using the G2MP2 method. There was no measurable amount of a parent ion U^-. We also report the occurrence of 12 other fragments produced by dissociative electron attachment to uracil but with lower cross sections than $(U\text{-}H)^-$. In addition we observed a parasitic contaminating process for conditions where uracil was introduced simultaneously with calibrant gases SF_6 and CCl_4 that leads to a sharp peak in the $(U\text{-}H)^-$ cross section close to 0 eV. For $(U\text{-}H)^-$ and all other fragments we determined rough measures for the absolute partial cross section yielding in the case of $(U\text{-}H)^-$ a peak value of σ (at 1.01 eV) $=3\times10^{-20}$ m^2. © *2004 American Institute of Physics.* [DOI: 10.1063/1.1649724]

INTRODUCTION

The noxious effect of ionizing radiation has been known since the discovery of radioactivity and x-rays. High energy radiation particles (α, β, γ, and heavy ions) ionize cell components along the radiation track, which leads to dissociation and formation of genotoxic radicals. A general introduction into the field of radiation damage from the medical–biological point of view (the steps from initial damage to the genome leading to mutations or up to growing of cancer tissue) can be found in Refs. 1 and 2. Today it is the accepted fact that one third of the damage is direct, i.e., from energy which is transferred into DNA and closely bound water molecules, while two-thirds of the damage is indirectly caused by radicals which are created via energy deposition in water molecules and other biomolecules surrounding the DNA.[3–5] Experiments of Folkard *et al.*[6] showed that photons in the energy range of 7–150 eV also induce single strand breaks (SSB) and double strand breaks (DSB) in dry plasmid DNA. They made also experiments with hydrated DNA and DNA in aqueous solution and observed enhanced damage. This was explained by the formation of the genotoxic OH radical because addition of an OH radical scavenger decreased the amount of strand breaks. Not only photons, also electrons with energy below the ionization threshold cause damage to DNA by forming mutagenic, recombinogenic, and lethal DNA and RNA lesions like single and double strand breaks. This observation has been made recently by Sanche and co-workers.[7] They showed that free electron attachment in a range between 3 and 20 eV induce SSBs and DSBs in DNA. The initial point of damage is the formation and the subsequent decay of transient negative ion states of various single components (base, deoxyribose, phosphate, and hydration water). When high energy radiation interacts with the cell environment, secondary electrons are produced in large amounts (4×10^4 electrons per 1 MeV deposited primary quantum)[8] with initial kinetic energies up to 20 eV.[9] They are thermalized within 10^{-12} s before they reach the stage of solvation (see also time resolved pulse radiolysis experiments with nucleotides, which demonstrate importance of presolvated electrons[10]).

The result of Sanche and co-workers shows the importance to study the intrinsic molecular behavior during free electron attachment to isolated gas-phase DNA/RNA molecules, i.e., electron energies for TNI formation, decay channels, etc. As a first step we have carried out experiments with uracil $C_4H_4N_2O_2$ [see Fig. 1(a) for molecular structure]. Uracil is one of the four bases of the RNA (the others are guanine, adenine and cytosine). RNA processes the information stored in DNA. Uracil is incorporated into a sugar-phosphate backbone and it always pairs with adenine by hydrogen bonding. More details about uracil and experiments with electron and proton ionization of uracil can be found in Ref. 11. To our knowledge there exists no previous measurement of dissociative electron attachment to isolated gas-phase uracil. In a previous letter[12] we briefly presented the first results of electron attachment to uracil; in the present paper our experimental results for uracil are discussed in detail.

In an early work Huels *et al.* mentioned the existence of stable parent anions formed by free electron attachment to DNA bases.[13] However, all following experiments including the group of Illenberger clearly revealed that the attachment of a free electron to DNA bases in gas phase leads exclusively to the formation of fragment anions.[14–16] The closed shell anions $(P\text{-}H)^-$ (P=pyrimidines: cytosine, thymine,

[a)]Author to whom correspondence should be addressed. Also adjunct professor at: Department of Plasma Physics, Comenius University, SK-84248 Bratislava, Slovakia. Electronic mail: tilmann.maerk@uibk.ac.at

and uracil) turn out to be the major reaction channel.

In addition several electron attachment experiments[17–20] have been carried out with substituted uracil (5-XU; X = Cl, F, Br, I, and 6-ClU), where one hydrogen is replaced by a halogen atom. Electron attachment to these halouracils leads to a detectable parent anion. For 5- and 6-ClU the most dominant reaction channel leads to the formation of $(U\text{-}HCl)^-$.[17–19] Aflatooni *et al.*[21] investigated temporary negative states of uracil by means of electron transmission spectroscopy (ETS), where electrons are populating empty π^* molecular orbitals. The formation of short lived anion states was detected at electron energies of 0.22, 1.58, and 3.83 eV. Since energy is needed to create these anion states, one can conclude, that the anion states are unstable against autodetachment (because the anion state is energetically higher in respect to energy). This result concerns only vertical transitions of the neutral state to the anion state within a Franck–Condon transition and not adiabatic transitions.

All experiments mentioned above only deal with valence bound anions (''conventional anions''), where the additional electron is populating a valence orbital. Another possibility for formation of an anion is binding of the extra electron in the dipole field of a molecule. Such dipole bound anions can be produced, if the dipole moment of the molecule is larger than 2.5 D. Like other pyrimidines, uracil has a high dipole moment of 4.3 D.[22] Thus it should be capable to produce dipole-bound anions where the electron is weakly bound far outside the molecular frame. Adamowicz and co-worker predict in theoretical calculations dipole-bound anions[22] for uracil. Schermann and co-workers[23] detected stable dipole-bound U-anions in Rydberg electron transfer with uracil and Bowen and co-workers observed these anions in negative ion photoelectron spectroscopy of uracil.[24] This is in agreement with Ref. 22, where a positive adiabatic electron affinity of EA = 86 meV was predicted. Schermann and co-workers also detected conventional valence bound anions, however, in this case the anion was not U^- but instead $(U\text{-}H)^-$. In a second experiment with mixed uracil–argon clusters Schermann and co-workers[25] were able to produce stable valence bound parent anions of uracil by Rydberg electron transfer. Such formation was possible when several argon atoms evaporated from a uracil–argon cluster. By using the same method Periquet *et al.*[26] estimated in a recent work the electron affinities of azine and DNA/RNA bases. Bowen and co-workers[27] investigated the transformation from dipole bound to covalent bound anions by negative ion photoelectron spectroscopy with different mixtures of uracil–X clusters (X = H_2O, Ar, Kr, Xe). In the case of an uracil–xenon complex, it is possible to observe simultaneously conventional and dipole-bound anions. Schied *et al.*[28] studied anion spectroscopy of uracil and of mixed uracil–H_2O clusters. They observed stabilization in uracil–H_2O clusters leading to valence bound anion states. By extrapolating the observed electron affinities for uracil–$(H_2O)_n$ clusters linearly to the bare uracil molecule they estimated the valence-bound EA to be 150 meV. There exist also theoretical studies on the determination of valence adiabatic and vertical electron affinities of DNA and RNA components.[29–32] All calculations give

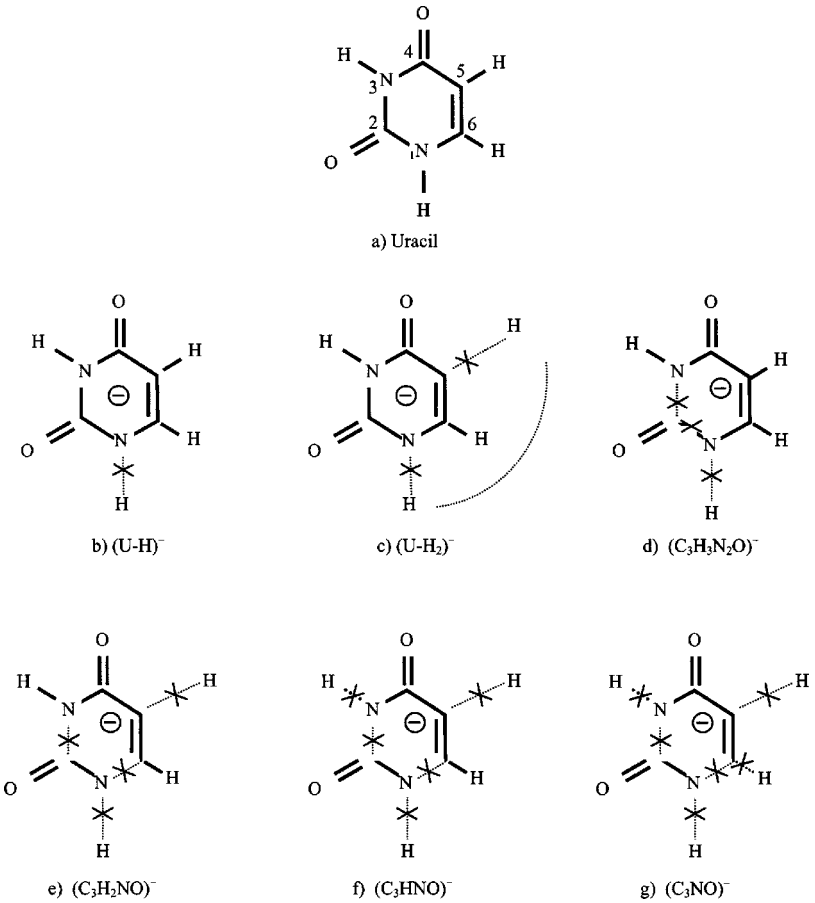

FIG. 1. (a) Structure formula of uracil and possible pathways for dissociation products in the mass region between 66 and 111 amu.

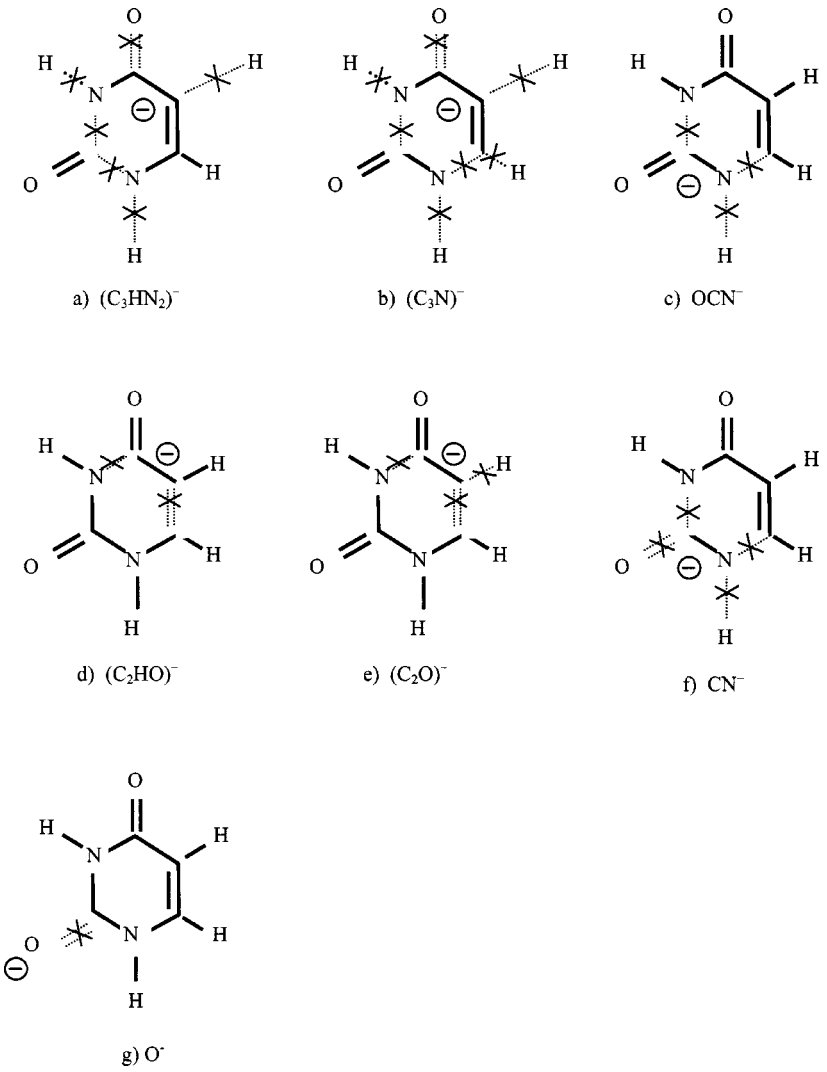

FIG. 1. (b) Possible pathways for dissociation products in the mass region between 16 and 65 amu.

a negative value for the vertical EA for the DNA bases. The adiabatic EA is very close to zero with slightly positive or negative value depending on the density function used for the calculation. Since all experiments and calculations predict a negative vertical electron affinity and a adiabatic EA near 0 eV, substantial relaxation of the nuclear framework of the uracil anion can be expected. This means that the structure of the equilibrated anion is significantly changed compared to the planar neutral molecule.[31]

EXPERIMENT

The apparatus used for the present measurements is a crossed electron–molecule beam-instrument developed in our laboratory in Innsbruck. A schematic view of this machine is shown in Fig. 2, a more detailed description can be found elsewhere.[33,34] The white uracil-powder (purity 99%, from Sigma-Aldrich) is heated up in a Knudsen type oven to a temperature of 185 °C. The temperature was measured with a PT100 resistance temperature sensor mounted at the oven. Through a capillary (diameter 1 mm) the gaseous uracil molecules are directly effused into the collision chamber of the hemispherical electron monochromator, where the interaction with the electron beam takes place. Maximum electron resolution of the monochromator is 35 meV, however, in order to achieve sufficient anion yield the energy resolution was kept here in a range between 90 and 120 meV. Negative ions that are formed by electron attachment to uracil are extracted on line from the collision chamber by a weak electric field (at maximum 200 meV/cm) and focused into a quadrupole mass spectrometer (maximum mass range 2048 amu). After mass selection the ions are detected by a channeltron type secondary electron multiplier. Using a pulse counting technique the ion yield was recorded as a function of the electron energy. The background base pressure in the main chamber was 10^{-6} Pa and was measured with an ionization gauge. During the measurements the main chamber was kept at a temperature of 100 °C to reduce condensation of uracil on lenses of the monochromator and quadrupole, which would deteriorate the performance of the instrument.

The energy scale and the energy resolution were determined using the s-wave electron attachment reaction to SF_6 or CCl_4.[35,36] The ion yield of SF_6^-/SF_6 or Cl^-/CCl_4 exhibits a sharp zero eV energy peak. The energy scale was calibrated relative to the position of this peak and from the corresponding full width at half maximum (FWHM) the energy resolution was determined. Furthermore the 0.8 eV peak of the

dissociative Cl^-/CCl_4 attachment reaction was used for determination of absolute partial cross section values. A requirement for exact determination is, that the ion yield of Cl^-/CCl_4 and the various uracil ion yields were measured under the same conditions, which means with same electron current, identical partial pressures, etc. (a detailed review, which discusses also discrimination due to kinetic energy release in dissociative attachment reaction, can be found in Ref. 37). The capillary used for the uracil measurements has a gas inlet connected to the CCl_4 container so that the calibration gas effuses parallel together with the molecular beam of uracil into the collision chamber. This arrangement can lead to further possible reactions between calibration gas and uracil molecules, which will be discussed below. By taking the known value of $\sigma = 5 \times 10^{-20}$ m^2 (Refs. 38, 39) for the cross section of Cl^-/CCl_4 at 0.8 eV, the cross section for the formation of uracil anions was determined, by comparing corresponding ion currents (see Ref. 37). The accuracy of this method can be estimated to be in the range of one order of magnitude.

RESULTS

Electron attachment to uracil has been studied in an electron energy range from about 0 to 14 eV. In our experiments we could detect the following reaction channels within our detection limit:

$$e + U \leftrightarrow (U)^{-*} \rightarrow (U\text{-}H)^- + H^{\bullet}, \quad (1a)$$

$$\rightarrow (U\text{-}2H)^- + 2H, \quad (1b)$$

$$\rightarrow (C_3H_3N_2O)^- + \text{fragments}, \quad (1c)$$

$$\rightarrow (C_3H_2NO)^- + \text{fragments}, \quad (1d)$$

$$\rightarrow (C_3HNO)^- + \text{fragments}, \quad (1e)$$

$$\rightarrow (C_3NO)^- + \text{fragments}, \quad (1f)$$

$$\rightarrow (C_3HN_2)^- + \text{fragments}, \quad (1g)$$

$$\rightarrow (C_3N)^- + \text{fragments}, \quad (1h)$$

$$\rightarrow (OCN)^- + \text{fragments}, \quad (1i)$$

$$\rightarrow (C_2H_3N)^- \text{ or } (C_2HO)^- + \text{fragments}, \quad (1j)$$

$$\rightarrow (C_2H_2N)^- \text{ or } (C_2O)^- + \text{fragments}, \quad (1k)$$

$$\rightarrow (CN)^- + \text{fragments}, \quad (1l)$$

$$\rightarrow (O)^- + \text{fragments}. \quad (1m)$$

A possible cleavage pathway for every anion observed is shown in Figs. 1(a) and 1(b). The ion yields for the corresponding anions are shown in Figs. 3–5 and in Tables I(a) and I(b) the positions of the peak resonances are listed. Using the calibration method mentioned above we estimated the absolute partial cross sections for all anion. The results are listed in Table II. Figure 6 shows the individual ion current for the three most abundant anions normalized to the total ion current as a function of the electron energy from 0 to 9 eV. It shows the efficiency of fragment formation as a function of the electron energy.

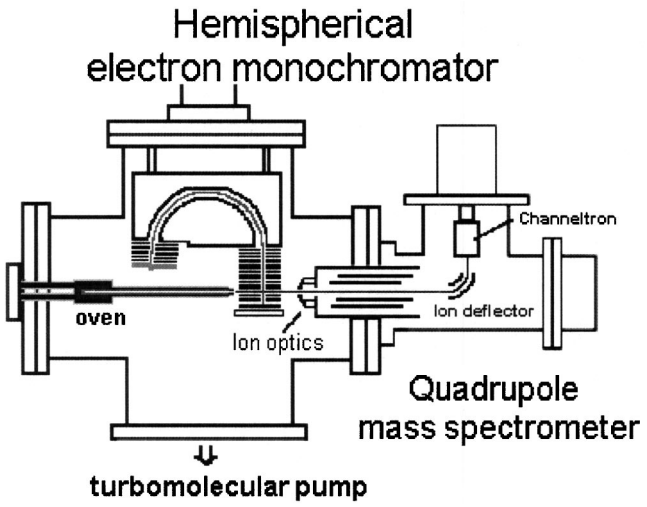

FIG. 2. Schematic view of the experimental setup.

In none of our free electron attachment experiments to uracil we have been able to detect a measurable amount of stable parent ion. Careful mass analysis shows that in fact there is a small signal at the mass of the parent ion. The measured ion yield at the parent mass has the same shape as one mass below but with much lower intensity. The calculated abundance for $(U\text{-}H)^-$ at parent mass due to the ^{13}C isotope (5.05%) fits with the experimental one within 1%, so this ion yield can be fully ascribed to the isotope peak of $(U\text{-}H)^-$. Theoretical calculations[29,30] and ETS[21] indicate a negative vertical electron affinity for uracil. Thus one can expect to observe no stable parent anion. This is in agreement with the experimental observation (please note that it is not possible to conclude from the nonobservation of a stable parent anion the occurrence of a negative EA, i.e., CCl_4[40] has a positive EA).

During our experiments we were confronted with an unexpected property of uracil in presence of an additional (calibrant) gas. Generally we use a mixture of calibration gas (CCl_4 or SF_6) and uracil to determine the exact peak position of the resonances in the uracil ion yield by measuring the calibration gas ion yield under the same experimental conditions. It turned out that such a mixture can cause problems because we assume that the following reactions between uracil and calibration gas occur:

$$U + Cl^- \rightarrow (U\text{-}H)^- + HCl, \quad (2a)$$

$$U + SF_6^- \rightarrow (U\text{-}H)^- + HF + SF_5, \quad (2b)$$

$$\rightarrow (U\text{-}2H)^- + 2HF + SF_4. \quad (2c)$$

In our opinion the neutral reaction product in reaction (2a) has to be HCl that is formed in an anion–neutral reaction. In the case of free electron attachment to 5-ClU[17,18] the most important reaction channel leads to $(5\text{-}ClU\text{-}HCl)^-$ close to zero eV electron energy. In this case the formation of two independent neutral radicals, i.e., $H^{\bullet}$ and $Cl^{\bullet}$ is from the energetic point of view not possible at this low electron energy. Using the same arguments the given neutral fragments for reactions (2b) and (2c) can be expected. All of these charge transfer reactions lead to an additional zero eV peak in the

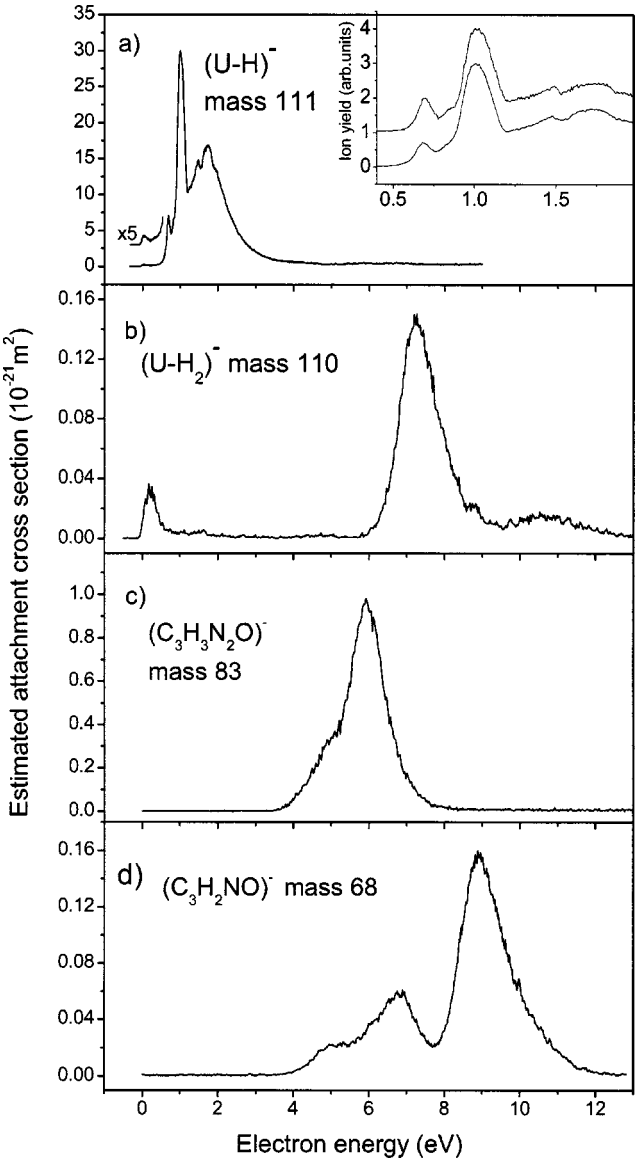

FIG. 3. Ion yield of $(U\text{-}H)^-$, $(U\text{-}H_2)^-$, $(C_3H_3N_2O)^-$, and $(C_3H_2NO)^-$ for dissociative electron attachment to uracil as a function of electron energy. These ion yields were measured without any presence of a calibration gas. The partial cross section scale was determined relative to the Cl^-/CCl_4 ion yield and has an accuracy within one order of magnitude. The inset in (a) shows the ion yield of $(U\text{-}H)^-$ measured at an electron energy resolution of 60 meV (upper curve) and 90 meV (lower curve), respectively.

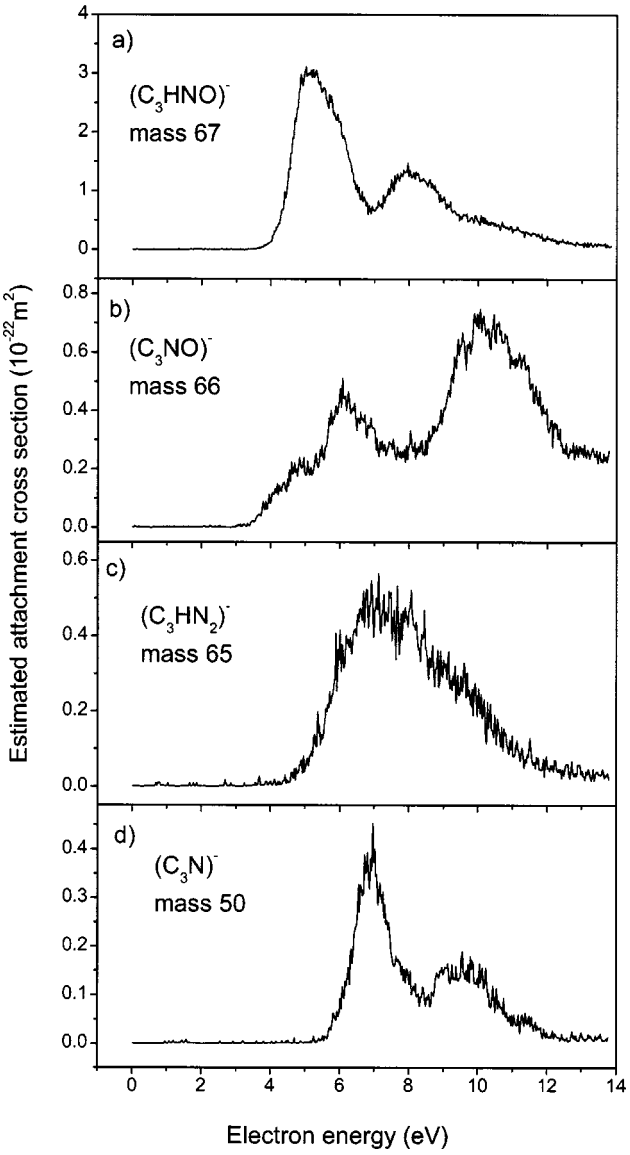

FIG. 4. Ion yield of $(C_3HNO)^-$, $(C_3NO)^-$, $(C_3HN_2)^-$, and $(C_3N)^-$ for dissociative electron attachment to uracil as a function of electron energy from about 0 to 14 eV. The partial cross section scale was determined relative to the Cl^-/CCl_4 ion yield and has an accuracy within one order of magnitude.

corresponding ion yield of $(U\text{-}H)^-$ or $(U\text{-}H_2)^-$. In Fig. 7 the ion yield of $(U\text{-}H)^-$ for different partial pressures of CCl_4 is shown. In Fig. 7(c), which was measured without calibration gas, the ion yield exhibits a small peak around 40 meV. With increasing partial pressure of CCl_4 [4×10^{-6} Pa in Fig. 7(b); 1.3×10^{-5} Pa in Fig. 7(a)] an additional peak grows in at zero eV. The artifact peak at zero eV increases nearly linearly with the partial pressure of the calibration gas (see Fig. 8). Artifact zero eV peaks have already been reported in electron attachment experiments to C_2Cl_4 by Drexel *et al.*[41] In these attachment experiments carried out with a trochoidal electron monochromator they observed for all fragment anions of C_2Cl_4 additional zero eV peaks and also in the O^-/O_2 ion yield, when C_2Cl_4 is present. $C_2Cl_4^-$ has a short lifetime of 14 μs against autodetachment, that means a substantial amount of electrons are released from metastable $C_2Cl_4^-$ in the μs time period. The flight time from the collision chamber to the quadrupole was estimated to be 50 μs. Hence they concluded that $C_2Cl_4^-$ was an electron carrier from the collision region to the quadrupole optic lens, where an electron detaches from the carrier, is accelerated and then may attach to form various fragment anions at a nominal zero eV electron energy. Such effects have been called by Ref. 41 ''Trojan horse ionization.'' In the present experiment only two fragment ions, i.e., $(U\text{-}H)^-$ and $(U\text{-}2H)^-$, exhibit an additional peak at zero eV, strongly depending on the partial pressure of the calibration gas. A reason for the surprisingly large yield of product anions formed by ion molecule reactions can be found in the experimental setup. Uracil vapor is coexpanded with the calibration

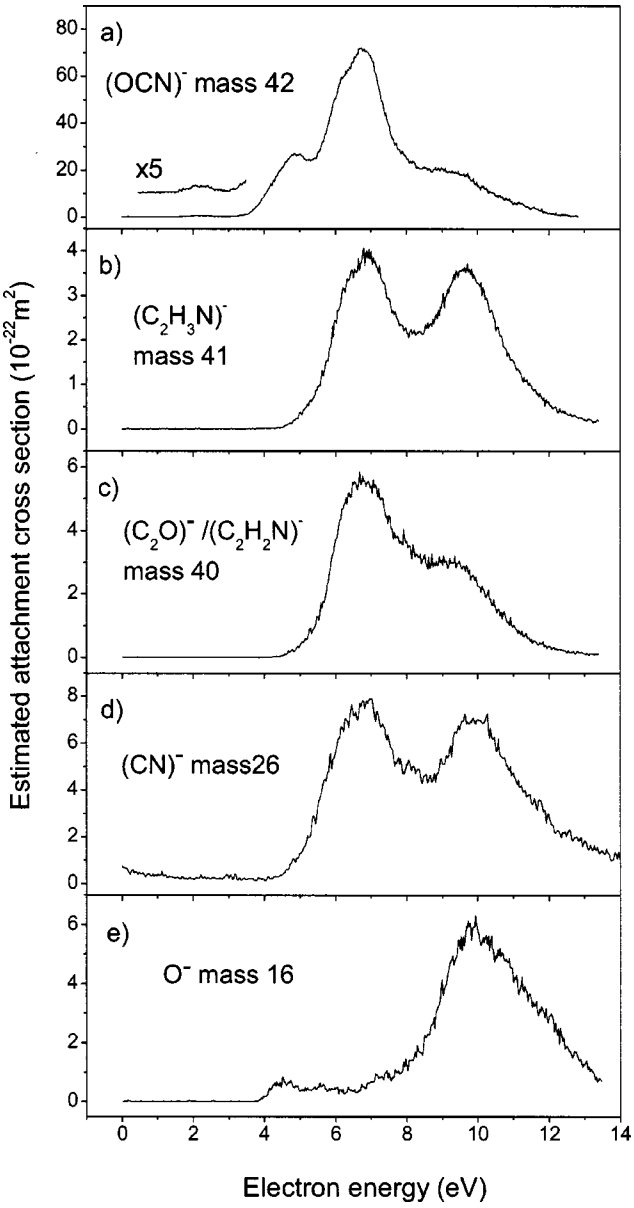

FIG. 5. Ion yield of $(OCN)^-$, $(C_2H_3N)^-/(C_2HO)^-$, $(C_2H_2N)^-/(C_2O)^-$, $(CN)^-$, and O^- for dissociative electron attachment to uracil as a function of electron energy from about 0 to 14 eV. The partial cross section scale was determined relative to the Cl^-/CCl_4 ion yield and has an accuracy within one order of magnitude.

gas through the capillary into the collision chamber. Both ions and neutrals leave the ion source towards the quadropole. The pressure in the collision region ($\sim 10^{-3}$ Pa) is several orders of magnitude higher than the measured pressure in the main chamber, thus large enough for intense ion–molecule reaction. In earlier measurements, when we introduced the calibration gas as a stagnant gas from the background gas inlet system into the chamber, we already observed this additional zero eV peak, although with lower intensity. Nevertheless it shows the high reactivity of uracil and the necessity to measure without any calibration gas to prevent such artifact peaks. For mass spectra recorded at an electron energy close to zero eV and with a mixture of SF_6 and uracil in the inlet additional reaction products appear at mass 130 and 131 amu (see Fig. 9).

$(C_4H_3N_2O_2)^-$ [$(U\text{-}H)^-$, 111 amu]

In Fig. 3(a) the ion yield at 111 amu [attributed to $(U\text{-}H)^-$] is shown measured without calibration gas. The corresponding resonances seen in Fig. 3(a) are listed in Table Ia. We have also performed measurements with a better electron energy resolution than our standard values of 90–120 meV in order to resolve the peak structure more accurately. The inset in Fig. 3(a) shows the peak structure of $(U\text{-}H)^-$ measured with the highest reachable energy resolution of about 60 meV during the experiments with uracil (upper curve) in comparison to the ion yield measured with 90 meV (lower curve). In addition to the peaks listed in Table Ia a small shoulder in the upper curve at an electron energy of 0.85 eV indicates the presence of a further peak, nevertheless the energy resolution is not sufficiently high to resolve this peak.

Electron affinities EA and the binding energies D(U-H) for uracil for the four possible isomeric (U-H) fragments were theoretically determined with *ab initio* calculations using the G2MP2[42] method with an uncertainty of about ± 0.1 eV.[42,43] From these data one can calculate the energy thresholds $E(n)$ for the formation of the different $(U\text{-}H)^-$ isomers:

$$E(n) = D(n) - EA(n) \quad (n = 1,3,5,6), \tag{3}$$

where n denotes the designated number of the carbon or nitrogen atom from which a hydrogen is removed [see Fig. 1(a)]. The results are listed in Table III. From these data we conclude that the energetically most favorable channel is hydrogen abstraction from ^{1}N. Although the calculated threshold is 0.8 eV, we already observe a first small peak around 40 meV. This energetically lowered peak position can be associated with a hot band transition, where attachment to a vibrationally excited neutral molecule occurs leading to $(U\text{-}H)^-$ formation.[44] The presently calculated EA of uracil using the G2MP2 method was obtained to be zero (the exact result is -0.02 eV) within the accuracy of the method and thus in good agreement with calculated values in the literature.[29–32] We further compared the equilibrium geometries [calculated with the second-order Möller–Plesset (MP2) method and the 6-31G(d) basis set] of U with those of the anions and the four neutral fragments (U-H). As expected, appreciable changes in the geometrical parameters were found but only U^- and the neutral U-H(3) (the hydrogen is removed from the nitrogen atom located at the position 3) turn out to be nonplanar molecules.

A possible explanation for some of the resonances is the formation of different $(U\text{-}H)^-$ isomers. The calculated threshold of 0.8 and 1.4 eV fits within the error with peak resonances at an electron energy of 0.7 and 1.48 eV in the ion yield of $(U\text{-}H)^-$. The largest peak at 1 eV and the resonance at 1.72 eV show again approximately the same distance in peak position, so this may be the formation of the same isomers but in this case via excited states. The formation of these isomers would only include the breaking of the ^{1}N–H and ^{3}N–H bond. With regard to the calculations there seems to be no indication of hydrogen dissociation from carbon atoms in the ion yield of $(U\text{-}H)^-$. This is in agreement with recent electron attachment experiments of Illenberger

TABLE I. Peak position of fragments formed via dissociative electron attachment to uracil in the mass region.

(a) between 66 and 111 amu

Resonance number	Ion					
	$(U\text{-}H)^-$	$(U\text{-}H_2)^-$	$(C_3H_3N_2O)^-$	$(C_3H_2NO)^-$	$(C_3HNO)^-$	$(C_3NO)^-$
1	0.04	0.1	5.92	5.24	5.17	4.95
2	0.69	7.22		6.05	7.96	6.07
3	1.01	10.59		6.75		10.33
4	1.48			8.97		
5	1.72					
6	1.89					

(b) between 16 and 65 amu

Resonance number	Ion						
	$(C_3HN_2)^-$	$(C_3N)^-$	$(OCN)^-$	$(C_2H_3N)^-/(C_2HO)^-$	$(C_2H_2N)^-/(C_2O)^-$	CN^-	O^-
1	7.13	6.92	2.22	6.85	6.8	6.79	4.55
2		9.49	4.92	9.65	9.08	9.89	5.64
3			6.29				10.4
4			6.73				
5			8.92				

and co-workers[45] with partially deuterated thymine. They observed only dehydrogenation from the nitrogen atoms. The broad peak at 1.72 eV is reminiscent of the formation of the anion state by occupation of the empty π^* valence orbital, i.e., ETS[21] shows a resonance at 1.58 eV. The cross section of the $(U\text{-}H)^-$ anion is 3×10^{-20} m^2 as listed in Table II, and it is the most abundant anion in electron attachment to uracil in the electron energy range from 0 to 3.9 eV (see Fig. 6).

$(C_4H_2N_2O_2)^-$ [$(U\text{-}2H)^-$, 110 amu]

The uracil fragment ion where two hydrogen atoms are missing, has a much lower cross section of 1.5×10^{-22} m^2 than $(U\text{-}H)^-$. The ion yield, shown in Fig. 3(b), reveals three peaks at 0.1, 7.22, and 10.59 eV. It is interesting to note, that the formation of this ion is also influenced by the presence of a calibration gas. This leads to the formation of a zero eV peak in the ion yield at mass 110 amu, which then overlaps with the first resonance at 0.1 eV. Apparently this anion is also produced via the charge transfer reaction described above, but in contrast to $(U\text{-}H)^-$ this effect can only be seen in the case of an admixture with SF_6 but not with CCl_4. The dependence of this zero peak on the presence of SF_6 was also determined and shows a linear behavior (see Fig. 8). Nevertheless also the peak near 0 eV without the presence of any calibration gas may be an artifact peak, since the relative peak height decreased slowly from day to day. A possible explanation is desorption of adlayers from the chamber walls of the apparatus resulting from earlier studies with 6-Chlorouracil. The ion with the highest abundance for 6-Chlorouracil is mass 110 amu $([6\text{-}ClU]\text{-}HCl)^-$ and the ion yield reveals a strong resonance close to zero eV.[19]

SMALL FRAGMENT ANIONS OF URACIL

In contrast to the previously described anions that are formed via removal of hydrogen atoms for smaller fragment

TABLE II. Estimated absolute partial cross section values for negative ions formed via dissociative electron attachment to uracil. The accuracy is within one order of magnitude.

Ion	Resonance (eV)	Cross section (m^2)
$(U\text{-}H)^-$	1.01	3×10^{-20}
$(U\text{-}H_2)^-$	7.22	1.5×10^{-22}
$(C_3H_3N_2O)^-$	5.92	9.8×10^{-22}
$(C_3H_2NO)^-$	8.97	1.63×10^{-21}
$(C_3HNO)^-$	5.17	3×10^{-22}
$(C_3NO)^-$	10.33	7×10^{-22}
$(C_3HN_2)^-$	7.13	5×10^{-23}
$(C_3N)^-$	6.92	4×10^{-23}
$(OCN)^-$	6.73	7.15×10^{-21}
$(C_2H_3N)^-$	6.85	3.8×10^{-22}
$(C_2H_2N)^-$–$(C_2O)^-$	6.8	5.8×10^{-22}
$(CN)^-$	6.79	8×10^{-22}
O^-	10.4	6.4×10^{-22}

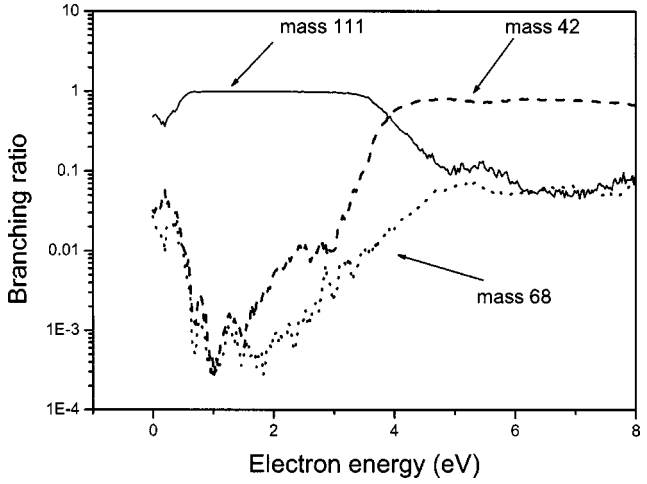

FIG. 6. Relative abundance of the three most intense anions $(U\text{-}H)^-$, $(C_3H_2NO)^-$, and $(OCN)^-$ for electron attachment to uracil.

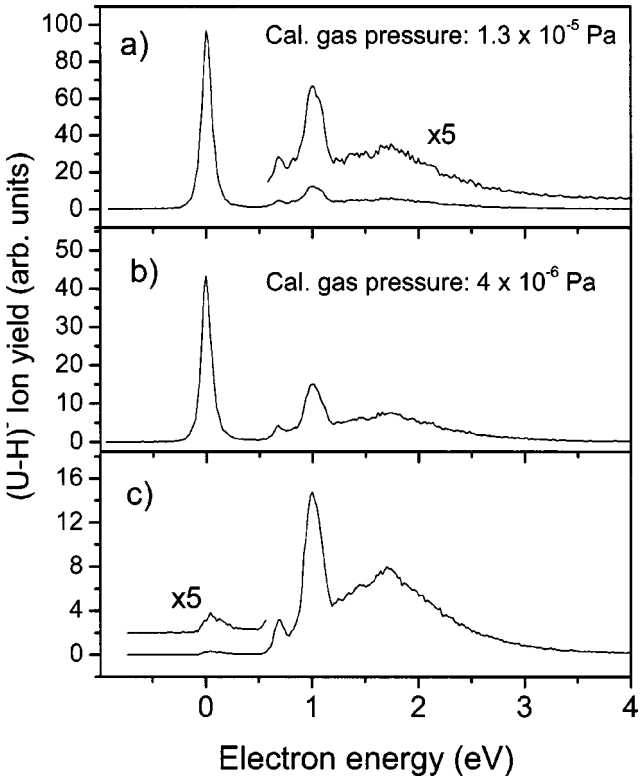

FIG. 7. $(U\text{-}H)^-$ ion yield as a function of electron energy for three different partial pressures of the calibration gas CCl_4 (pressure is read on ionization gauge in main chamber), (c): no calibration gas, (b): 4×10^{-6} Pa, (a): 1.3×10^{-5} Pa.

ions much stronger bonds have to be broken. This is reflected in the high electron energies, i.e., typically higher than 4 eV, of the observed resonances of these anions. Tables I(a) and I(b) summarize the peak positions of all identified resonances and in Table II the maximum value of the estimated partial cross sections are listed. By comparing the ion yields in Figs. 3–5 and the position of the corresponding resonances one can see that these fragments have very similar resonances with respect to the position although the ratio of

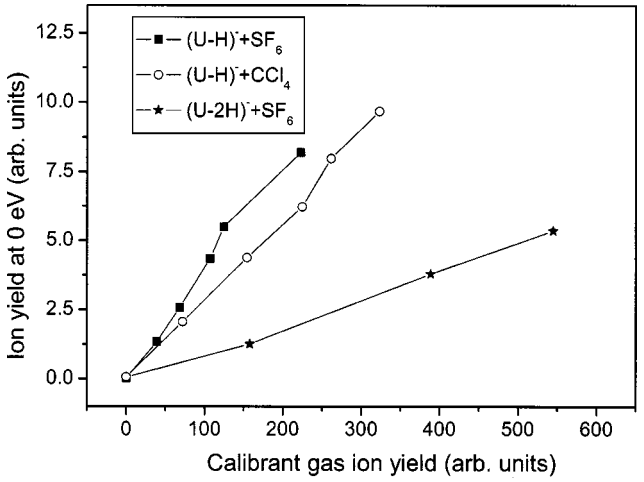

FIG. 8. $(U\text{-}H)^-$ ion signal at zero eV electron energy as a function of calibrant anion signal for SF_6 (filled squares) and CCl_4 (open circles) and $(U\text{-}2H)^-$ ion signal as a function for SF_6 (filled star).

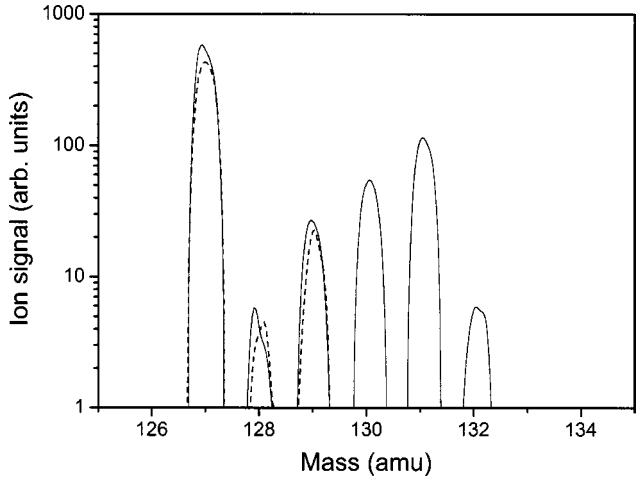

FIG. 9. Mass spectra in the range from 125 to 135 amu of a mixture of uracil–SF_6 (full line) and pure SF_6 (dotted line) at zero eV electron energy. The peak at 127 amu can be ascribed to SF_5^- and the corresponding isotope peaks can be detected at 128 and 129 amu. The peaks at 130 and 131 amu (with detected isotope peak at 132 amu) can only be observed in the presence of SF_6 and uracil.

the peak heights is different. These similar peak positions may be due to the formation of a common precursor states $U^{-}*$ which then dissociates into one of these competitive reaction channels. The different relative peak heights indicate that competing channels have different reaction probabilities at different electron energies. For example, the ion yield of the two fragment anions $(C_3H_2NO)^-$ (68 amu) and $(OCN)^-$ (42 amu) show common resonances [except the first very weak resonance of $(OCN)^-$] at five different electron energies. It is interesting to note that these two fragments combined form the intact uracil molecule except for one missing hydrogen at both anions. Remarkable is, that $(OCN)^-$ is the most abundant anion of all formed anions, for electron energies larger than 3.9 eV (see Fig. 6). Also most of the ions shown in Fig. 5 have common resonances at an electron energy of about 7 eV [Figs. 5(a)–5(d)] and 10 eV [Figs. 5(b)–5(e)].

SUMMARY AND CONCLUSION

We performed electron attachment experiments with isolated gas-phase uracil with a hemispherical electron monochromator in an electron energy range between about 0 and 14 eV. The anion with the highest abundance is $(U\text{-}H)^-$ with a maximum cross section of 3×10^{-20} m^2. Quantum chemical calculations predict that the calculated threshold energy

TABLE III. Calculated bond energies (U-H)-H and electron affinities for different U-H isomers. From difference of these values threshold energies for the different isomers of $(U\text{-}H)^-$ can be determined.

Position of H-atom	Bond energy (U-H)-H (eV)	Electron affinity EA for U-H (eV)	Energy threshold for $(U\text{-}H)^-$ (eV)
^{1}N–H	4.4	3.6	0.8
^{3}N–H	5.4	4.0	1.4
^{5}C–H	5.2	2.5	2.7
^{6}C–H	5.0	2.8	2.2

for the formation of this anion is 0.8 eV. Nevertheless we already observe $(U\text{-}H)^-$ at lower electron energies, probably due to vibrationally excited neutral molecules. Beside $(U\text{-}H)^-$ and $(U\text{-}2H)^-$ we observed 11 fragment ions formed by dissociation of the aromatic ring of the uracil molecule. We also studied the high reactivity of the uracil molecule in presence of a calibration gas, which leads to additional 0 eV peaks in the ion yield of $(U\text{-}H)^-$ and $(U\text{-}2H)^-$. This reaction can be explained as charge transfer ion molecule reactions between calibration gas anions and neutral uracil molecules. Thus it is absolutely necessary to measure without the presence of any (calibration) gas to avoid artifact peaks.

The present experiments can be seen as a first step in the investigation of damage to DNA–RNA components due to low energy secondary electrons. One main observation of nearly all free electron attachment experiments to isolated gas-phase biomolecules (DNA–RNA bases,[14–16] amino acids like glycine[46,47]) is the absence of parent ions M^- and the formation of a closed shell anion $(M\text{-}H)^-$. An open question can be how relevant are our results for real cell systems. One can conclude, since the translational excess energy of the transient negative ion after electron attachment to uracil will be nearly completely transferred into the mobile hydrogen radical in the case of $(U\text{-}H)^-$ formation that dissociative attachment stays important also in a complex cell structure. This nearly complete transfer will happen due to the linear momentum conservation ($>$99%).

Nevertheless one has to consider that the present experiment is electron attachment to isolated gas phase molecules. Electron attachment to uracil embedded in RNA may lead to different reactions, i.e., dissipation of the energy into neighboring molecules is possible, thus preventing dissociation. Theoretical calculations by Wetmore *et al.* already come to this conclusion,[48] because they observed positive vertical and adiabatic electron affinity for uracil in solution. So the solution stabilizes the anion preventing autodetachment from the electron from the uracil anion. For mixed clusters with uracil this has been already observed experimentally.[25–27]

ACKNOWLEDGMENTS

This work has been supported by the FWF, and ÖNB, Wien, Austria, and European Commission, Brussels.

[1] W. Dekant and S. Vamvakas, *Toxikologie* (Spektrum Akademischer Verlag, Heidelberg, 1994).
[2] A. L. Lehninger, *Biochemistry* (Worth, New York, 1970).
[3] B. D. Michael and P. A. O'Neill, Science **287**, 1603 (2000).
[4] C. M. DeLara, T. J. Jenner, K. M. S. Townsend, S. J. Marsden, and P. O'Neill, Radiat. Res. **144**, 43 (1995).
[5] J. K. Wolken, E. A. Syrstad, S. Vivekananda, and F. Turicek, J. Am. Chem. Soc. **123**, 5804 (2001).
[6] M. Folkard, K. M. Prise, B. Brocklehurst, and B. D. Michael, J. Phys. B **32**, 2753 (1999).
[7] B. Boudaiffa, P. Cloutier, D. Hunting, M. A. Huels, and L. Sanche, Science **287**, 1658 (2000).
[8] 1. International Commission on Radiation Units and Measurements, *ICRU Report 31* (ICRU, Washington, DC, 1979).
[9] V. Cobut, Y. Fongillo, J. P. Patau, T. Goulet, M.-J. Fraser, and J.-P. Jay-Gerin, Radiat. Phys. Chem. **51**, 229 (1998).
[10] J. E. Aldrich, K. Y. Lam, P. C. Shragge, and J. W. Hunt, Radiat. Res. **63**, 42 (1975).
[11] B. Coupier, B. Farizon, M. Farizon, *et al.*, Eur. Phys. J. D **20**, 459 (2002).
[12] G. Hanel, B. Gstir, S. Denifl, P. Scheier, M. Probst, B. Farizon, M. Farizon, E. Illenberger, and T. D. Märk, Phys. Rev. Lett. **90**, 188104-1 (2003).
[13] M. A. Huels, I. Hahndorf, E. Illenberger, and L. Sanche, J. Chem. Phys. **108**, 1309 (1998).
[14] S. Gohlke and E. Illenberger, Europhys. News **33**, 207 (2002).
[15] S. Denifl, S. Ptasińska, M. Cingel, S. Matejcik, P. Scheier, and T. D. Märk, Chem. Phys. Lett. **377**, 74 (2003).
[16] R. Abouaf, J. Pommier, and H. Dunet, Int. J. Mass. Spectrom. **226**, 397 (2003).
[17] S. Denifl, S. Matejcik, B. Gstir, G. Hanel, M. Probst, P. Scheier, and T. D. Märk, J. Chem. Phys. **118**, 4107 (2003).
[18] H. Abdoul-Carime, M. A. Huels, E. Illenberger, and L. Sanche, Int. J. Mass. Spectrom. **228**, 703 (2003).
[19] S. Denifl, S. Ptasińska, S. Matejcik, E. Illenberger, P. Scheier, and T. D. Märk, Int. J. Mass Spectrometry (to be published).
[20] H. Abdoul-Carime, M. A. Huels, F. Brüning, E. Illenberger, and L. Sanche, J. Chem. Phys. **113**, 2517 (2000).
[21] K. Aflatooni, G. A. Gallup, and P. D. Burrow, J. Phys. Chem. **102**, 6205 (1998).
[22] N. A. Oyler and L. Adamowicz, J. Phys. Chem. **97**, 11122 (1993).
[23] C. Desfrancois, H. Abdoul-Carime, and J. P. Schermann, J. Chem. Phys. **104**, 7792 (1996).
[24] J. H. Hendricks, S. A. Lyapustina, H. L. de Clercq, J. T. Snodgrass, and K. H. Bowen, J. Chem. Phys. **104**, 7788 (1996).
[25] C. Desfrancois, V. Periquet, Y. Bouteilleir, and J. P. Schermann, J. Phys. Chem. **102**, 1274 (1998).
[26] V. Periquet, A. Moreau, S. Carles, J. P. Schermann, and C. Desfrancois, J. Electron Spectrosc. Relat. Phenom. **106**, 141 (2000).
[27] J. H. Hendricks, S. A. Lyapustina, H. L. de Clercq, and K. H. Bowen, J. Chem. Phys. **108**, 8 (1998).
[28] J. Schiedt, R. Weinkauf, D. M. Neumark, and E. W. Schlag, Chem. Phys. **239**, 511 (1998).
[29] A. O. Colson and M. D. Sevilla, Int. J. Radiat. Biol. **67**, 627 (1995).
[30] S. D. Wetmore, R. J. Boyd, and L. A. Eriksson, Chem. Phys. Lett. **322**, 129 (2000).
[31] S. S. Wesolowski, M. L. Leininger, P. N. Pentchev, and H. F. Schaefer III, J. Am. Chem. Soc. **123**, 4023 (2001).
[32] N. Russo, M. Toscano, and A. Grand, J. Comput. Chem. **21**, 1243 (2000).
[33] D. Muigg, G. Denifl, A. Stamatovic, and T. D. Märk, Chem. Phys. **239**, 409 (1998).
[34] G. Hanel, T. Fiegele, A. Stamatovic, and T. D. Märk, Int. J. Mass. Spectrom. **205**, 65 (2001).
[35] S. Matejcik, G. Senn, P. Scheier, A. Kiendler, A. Stamatovic, and T. D. Märk, J. Chem. Phys. **107**, 8955 (1997).
[36] G. Senn, J. D. Skalny, A. Stamatovic, N. J. Mason, P. Scheier, and T. D. Märk, Phys. Rev. Lett. **82**, 5028 (1999).
[37] P. Cicman, M. Francis, J. D. Skalny, and T. D. Märk, Int. J. Mass. Spectrom. **223/224**, 271 (2003), and references therein.
[38] S. C. Chu and P. D. Burrow, Chem. Phys. Lett. **172**, 17 (1990).
[39] D. Klar, M.-W. Ruf, H. Hotop, Int. J. Mass. Spectrom. **205**, 93 (2001).
[40] E. Illenberger, *Gaseous Molecular Ions, Topics in Physical Chemistry, Vol. 2*, edited by H. Baumgaertl, E. U. Frank, and W. Gruebein (Steinkopff Verlag, Darmstadt, Springer, New York, 1992).
[41] H. Drexel, W. Sailer, V. Grill, P. Scheier, E. Illenberger, and T. D. Märk, J. Chem. Phys. **118**, 7394 (2003).
[42] L. A. Curtiss, K. Raghavachari, and J. A. Pople, J. Chem. Phys. **98**, 1293 (1993).
[43] R. D. Bach, P. Y. Ayala, and H. B. Schlegel, J. Am. Chem. Soc. **118**, 12758 (1996).
[44] I. Hahndorf and E. Illenberger, Int. J. Mass. Spectrom. **167/168**, 87 (1997).
[45] S. Gohlke, H. Abdoul-Carime, and E. Illenberger, International Symposium on Electron–Molecule Collisions and Swarms, Pruhonice near Prague, 2003.
[46] S. Gohlke, A. Rosa, E. Illenberger, F. Brünig, and M. A. Huels, J. Chem. Phys. **116**, 10164 (2002).
[47] S. Ptasińska, S. Denifl, A. Abedi, P. Scheier, and T. D. Märk, Chem. Phys. Lett. **377**, 74 (2003).
[48] S. D. Wetmore, R. J. Boyd, and L. A. Eriksson, Chem. Phys. Lett. **343**, 151 (2001).